

rearrangement is involved in the transformation of eq 1.

The synthetic and structural principles of heterometallic alkoxide chemistry reported here should generalize to other large divalent cations such as lead or strontium as precursors for the zirconates of these metals. Additionally, while  $\text{BaZrO}_3$  is cubic, the synthetic principles reported here should be useful in leading to ferroelectric  $\text{BaTiO}_3$  and to antiferroelectric  $\text{PbZrO}_3$ .

**Acknowledgment.** This work was supported by the Department of Energy. We thank Scott Horn for skilled technical assistance.

**Supplementary Material Available:** For 1 and 2, tables listing full crystallographic details, anisotropic thermal parameters, and bond distances and angles and a figure showing atom labeling (9 pages); tables of observed and calculated structure factors (21 pages). Ordering information is given on any current masthead page.

Contribution from the Department of Chemistry and Laboratory for Molecular Structure and Bonding, Texas A&M University, College Station, Texas 77843

## Ring Opening of the $[\text{Au}(\text{CH}_2)_2\text{PPh}_2]_2\text{X}_4$ ( $\text{X} = \text{Halogen}$ ) Metallacycle. Cleavage of $\text{Au}^{\text{III}}-\text{CH}_2$ Bonds

Raphael G. Raptis, John P. Fackler, Jr.,\* John D. Basil, and Douglas S. Dudis

Received March 29, 1991

The reactions of  $[\text{Au}(\text{CH}_2)_2\text{PPh}_2]_2$  (**1**) with excess  $\text{ICl}$  and  $\text{Br}_2$  initially give the  $\text{Au}^{\text{III}}$  tetrahalide complexes  $[\text{Au}(\text{CH}_2)_2\text{PPh}_2]_2\text{X}_4$  ( $\text{X} = \text{Cl}$  (**2**) or  $\text{Br}$  (**3**), respectively). Further reaction cleaves an  $\text{Au}^{\text{III}}-\text{CH}_2$  bond to form the ring-opened dimers  $\text{Cl}_3\text{Au}[\mu-(\text{CH}_2)_2\text{PPh}_2]\text{AuCl}_2(\text{CH}_2\text{PPh}_2\text{CH}_2\text{I})$  (**4**) and  $\text{Br}_3\text{Au}[\mu-(\text{CH}_2)_2\text{PPh}_2]\text{AuBr}_2(\text{CH}_2\text{PPh}_2\text{CH}_2\text{Br})$  (**5**). Complexes **4** and **5** have been characterized by single-crystal X-ray crystallography: for **4**, monoclinic,  $P2_1/n$ ,  $a = 10.322$  (2) Å,  $b = 23.592$  (4) Å,  $c = 15.516$  (2) Å,  $\beta = 103.68$  (1)°,  $V = 3671$  (1) Å<sup>3</sup>,  $Z = 4$ , refinement of 202 parameters with 2790 observed reflections gave  $R = 0.043$  and  $R_w = 0.039$ ; for **5**, monoclinic,  $P2_1/n$ ,  $a = 10.392$  (2) Å,  $b = 23.850$  (5) Å,  $c = 15.964$  (3) Å,  $\beta = 103.17$  (2)°,  $V = 3853$  Å<sup>3</sup>,  $Z = 4$ , refinement of 211 parameters with 1668 observed reflections gave  $R = 0.058$  and  $R_w = 0.055$ .

### Introduction

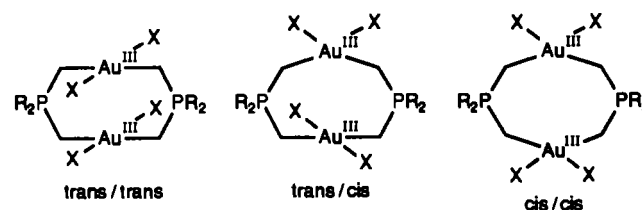
The dimeric  $\text{Au}^{\text{I}}$  complex<sup>1</sup>  $[\text{Au}(\text{CH}_2)_2\text{PPh}_2]_2$  (**1**) undergoes a two-<sup>2</sup> or four-electron<sup>2h,3</sup> oxidative-addition reaction to form  $\text{Au}^{\text{II}}$  or  $\text{Au}^{\text{III}}$  species, respectively. Dimers with both gold(III) centers containing halides in trans,<sup>3</sup> in cis,<sup>4</sup> or in one trans and one cis geometry<sup>3b,c</sup> have been characterized structurally (Chart I). Isomerization reactions<sup>3b,4</sup> between these various isomers have been observed.

The reaction of **1** with methylene halides gives<sup>2d,e,5</sup>  $\mu\text{-CH}_2$  "A-frame" products. The bridging ylide ligand  $(\text{CH}_2)_2\text{PPh}_2^-$  does not appear to participate in this chemistry. It preserves the dimeric nature of the complexes by holding the two gold atoms in close proximity. The stability<sup>6</sup> of the  $\text{Au}-\text{C}$  bonds is enhanced by the presence of the ylide phosphonium center. The reaction chemistry of **1** is attributed to the proximity of the Au centers across the ylide ligand, which has a bite of  $\sim 3.0$  Å. In the case of its  $\text{Au}^{\text{III}}$  derivatives, this  $\text{Au}\cdots\text{Au}$  interaction causes a severe distortion of the geometry<sup>7</sup> of the  $d^8$  metal atoms.

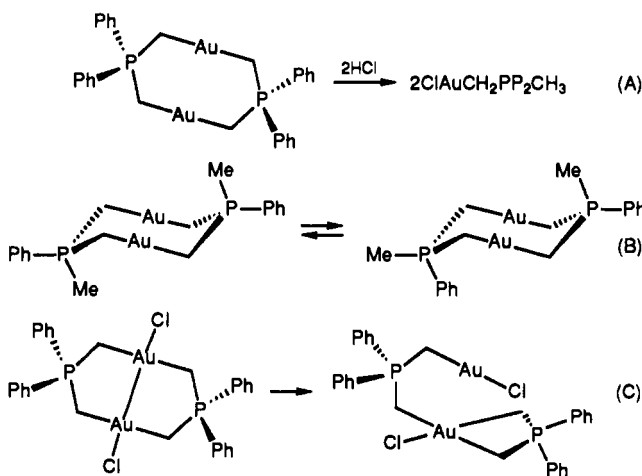
Three notable reactions have been observed in the chemistry of **1** and its derivatives wherein the ylide is an active component in the chemical processes. The reaction<sup>8</sup> of **1** with  $\text{HCl}$  (eq A of Scheme I) cleaves symmetrically two  $\text{Au}-\text{CH}_2$  bonds thus breaking down the dimer into two monomeric  $\text{Au}^{\text{I}}$ -ylide fragments. The methyl phenyl analogue to **1**,  $[\text{Au}(\text{CH}_2)_2\text{PMePh}]_2$ , isomerizes<sup>9</sup> between its cis and trans geometrical forms (eq B), a process that cleaves and re-forms  $\text{Au}-\text{CH}_2$  bonds. In polar solvents the  $\text{Au}^{\text{II}}$  complex  $[\text{Au}(\text{CH}_2)_2\text{PPh}_2]_2\text{Cl}_2$  disproportionates<sup>10</sup> (eq C) to a mixed-valence,  $\text{Au}^{\text{I}}/\text{Au}^{\text{III}}$  complex with one ylide ligand bridging the two gold atoms and the other chelating. In the case of the  $d^8$   $\text{Au}^{\text{III}}$  compounds of this ylide dimer system, the  $\text{CH}_2-\text{Au}$   $\sigma$  bonds appear to be less labile. Reactions involving the cleavage of these  $\text{Au}-\text{CH}_2$  bonds have not been described prior to this work.

In this paper we report that the  $\text{Au}^{\text{III}}-\text{CH}_2$  bonds of the complexes  $[\text{Au}(\text{CH}_2)_2\text{PPh}_2]_2\text{X}_4$ , ( $\text{X} = \text{Cl}$  (**2**),  $\text{Br}$  (**3**)) can be cleaved by polar oxidizing agents or by prolonged reaction with halogens. The ring-opened dimeric complexes  $\text{Cl}_3\text{Au}[\mu-(\text{CH}_2)_2\text{PPh}_2]\text{AuCl}_2(\text{CH}_2\text{PPh}_2\text{CH}_2\text{I})$  (**4**) and  $\text{Br}_3\text{Au}[\mu-(\text{CH}_2)_2\text{PPh}_2]\text{AuBr}_2(\text{CH}_2\text{PPh}_2\text{CH}_2\text{Br})$  (**5**) have been characterized crystallographically.

Chart I



Scheme I



( $\text{CH}_2\text{PPh}_2\text{CH}_2\text{Br}$ ) (**5**) have been characterized crystallographically.

- (1) (a) Cotton, F. A.; Wilkinson, G. *Advanced Inorganic Chemistry*, 5th ed.; John Wiley and Sons: New York, 1990; pp 949-950. (b) Basil, J. D.; Murray, H. H.; Fackler, J. P., Jr.; Tocher, J.; Mazany, A. M.; Trzcińska-Bancroft, B.; Knachel, H.; Dudis, D.; Delord, T. J.; Marler, D. O. *J. Am. Chem. Soc.* **1985**, *107*, 6908. (c) Schmidbaur, H.; Mandl, J. R.; Frank, A.; Huttner, G. *Chem. Ber.* **1976**, *109*, 466-472. (d) See also: Jones, P. G. *Gold Bull.* **1981**, *14*, 159-166. Schmidbaur, H. *Angew. Chem., Intl. Ed. Engl.* **1983**, *22*, 907. Schmidbaur, H.; Hartman, C.; Rebev, G.; Müller, G. *Angew. Chem., Intl. Ed. Engl.* **1987**, *26*, 1146.

\*To whom correspondence should be addressed.

Table I. Crystallographic Data for 4 and 5

	4	5
formula	$\text{C}_{29}\text{H}_{30}\text{Au}_2\text{Cl}_7\text{IP}_2$	$\text{C}_{29}\text{H}_{29}\text{Au}_2\text{Br}_6\text{Cl}_3\text{P}_2$
fw	1209.52	1420.20
space group	$P2_1/n$ (No. 14)	$P2_1/n$ (No. 14)
<i>a</i> , Å	10.322 (2)	10.392 (2)
<i>b</i> , Å	23.592 (4)	23.850 (3)
<i>c</i> , Å	15.516 (2)	15.964 (3)
$\beta$ , deg	103.68 (1)	103.17 (2)
<i>V</i> , Å <sup>3</sup>	3671 (1)	3853 (1)
<i>Z</i>	4	4
$d_{\text{calc}}$ , g cm <sup>-3</sup>	2.19	2.45
$\mu$ (Mo K $\alpha$ ), cm <sup>-1</sup>	94.23	140.74
radiation $\lambda$ , Å (monochromated in Mo K $\alpha$ incident beam)	0.710 69	0.710 69
temp, °C	22	22
<i>R</i> <sup>a</sup>	0.043	0.058
<i>R</i> <sub>w</sub> <sup>b</sup>	0.039	0.055

$$^a R = \sum ||F_o| - |F_c|| / \sum |F_o|. \quad ^b R_w = [\sum w^{1/2}(|F_o| - |F_c|)] / \sum w^{1/2}|F_o|; w^{-1} = [\sigma^2(|F_o|) + |g|F_o^{-2}].$$

### Experimental Section

**Synthesis of  $\text{Cl}_3\text{Au}[\mu-(\text{CH}_2)_2\text{PPh}_2]_2\text{AuCl}_2(\text{CH}_2\text{PPh}_2\text{CH}_2\text{I})$  (4).** To 15 mg (0.018 mmol) of **1** (prepared by a literature procedure<sup>1</sup>) in 2 mL of  $\text{CH}_2\text{Cl}_2$  was added 0.2 mL (0.2 mmol) of a 1.0 M solution of ICl. The solution turned dark red and was stirred for 3 h. The solvent, excess ICl, and free I<sub>2</sub> were removed under vacuum leaving an orange-yellow solid. Slow diffusion of Et<sub>2</sub>O into a  $\text{CH}_2\text{Cl}_2$  solution of this product afforded in good yield yellow crystals of **4** appropriate for X-ray diffraction study.

**Synthesis of  $\text{Br}_2\text{Au}[\mu-(\text{CH}_2)_2\text{PPh}_2]_2\text{AuBr}_2(\text{CH}_2\text{PPh}_2\text{CH}_2\text{Br})$  (5).** Crystals of **5** were obtained by evaporation of a  $\text{CDCl}_3$  solution of **3** (obtained by the addition of Br<sub>2</sub> to **1**) and Br<sub>2</sub>. In addition to the yellow crystals of **5** and the orange crystals of **3**, other unidentified materials were formed.

### X-ray Crystallography

The X-ray analyses of **4** and **5** were carried out with a Nicolet R3m/E automated four-circle diffractometer and SHELXTL software implemented on an Eclipse S140 minicomputer. Single crystals appropriate for X-ray study were mounted atop glass fibers at random orientation for data collection. Initial cell parameters were determined by using orientation reflections obtained from photographic data and were confirmed by axial photographs and a Delaunay reduction. Accurate unit cell dimensions were calculated from the setting angles of high-angle reflections. The intensity data were corrected for Lorentz and polarization effects and standard decay. An empirical absorption correction based on azimuthal

Table II. Atomic Coordinates ( $\times 10^4$ ) and Isotropic Thermal Parameters ( $\text{\AA}^2 \times 10^3$ ) for  $\text{Cl}_3\text{Au}[\mu-(\text{CH}_2)_2\text{PPh}_2]_2\text{AuCl}_2(\text{CH}_2\text{PPh}_2\text{CH}_2\text{I})\cdot\text{CH}_2\text{Cl}_2$  (4)

atom	<i>x</i>	<i>y</i>	<i>z</i>	<i>U</i> <sub>iso</sub> <sup>a</sup>
Au(1)	9478 (1)	1795 (1)	8633 (1)	47 (1)*
Au(2)	3213 (1)	71 (1)	7630 (1)	47 (1)*
I	6538 (1)	-670 (1)	5998 (1)	75 (1)*
Cl(1)	1238 (5)	2387 (2)	8751 (3)	84 (2)*
Cl(2)	-1942 (5)	2562 (2)	8733 (4)	85 (3)*
Cl(3)	-2202 (4)	1153 (2)	8541 (3)	73 (2)*
Cl(4)	3275 (5)	64 (2)	6176 (3)	82 (2)*
Cl(5)	3101 (5)	67 (2)	9082 (3)	71 (2)*
P(1)	899 (4)	1020 (2)	7418 (3)	47 (2)*
P(2)	5737 (4)	-818 (2)	7911 (3)	43 (2)*
C(1)	10710 (15)	1129 (7)	8528 (9)	52 (7)*
C(2)	1182 (15)	278 (7)	7263 (10)	54 (7)*
C(3)	5281 (15)	-96 (6)	7993 (11)	51 (7)*
C(4)	5384 (15)	-1065 (6)	6785 (9)	46 (7)*
C(11)	13357 (11)	1554 (5)	7867 (5)	62 (5)
C(12)	14499 (11)	1780 (5)	7665 (5)	86 (6)
C(13)	14542 (11)	1864 (5)	6782 (5)	71 (5)
C(14)	13444 (11)	1722 (5)	6101 (5)	70 (5)
C(15)	12303 (11)	1496 (5)	6303 (5)	62 (5)
C(16)	12259 (11)	1412 (5)	7186 (5)	50 (5)
C(21)	9217 (9)	1807 (4)	6398 (6)	58 (5)
C(22)	8018 (9)	1978 (4)	5835 (6)	68 (5)
C(23)	7001 (9)	1585 (4)	5541 (6)	65 (5)
C(24)	7182 (9)	1020 (4)	5810 (6)	70 (6)
C(25)	8381 (9)	849 (4)	6373 (6)	50 (5)
C(26)	9399 (9)	1242 (4)	6667 (6)	42 (4)
C(31)	18296 (11)	-467 (4)	8728 (7)	56 (5)
C(32)	19655 (11)	-555 (4)	9078 (7)	63 (5)
C(33)	20190 (11)	-1099 (4)	9093 (7)	71 (6)
C(34)	19365 (11)	-1555 (4)	8758 (7)	88 (7)
C(35)	18005 (11)	-1468 (4)	8409 (7)	85 (6)
C(36)	17471 (11)	-924 (4)	8394 (7)	44 (4)
C(41)	13840 (11)	-1639 (5)	8032 (6)	70 (6)
C(42)	13130 (11)	-1964 (5)	8515 (6)	82 (6)
C(43)	13391 (11)	-1909 (5)	9435 (6)	78 (6)
C(44)	14362 (11)	-1529 (5)	9872 (6)	109 (8)
C(45)	15071 (11)	-1204 (5)	9390 (6)	94 (7)
C(46)	14810 (11)	-1259 (5)	8469 (6)	48 (4)
C*	-653 (37)	1159 (13)	3419 (23)	327 (30)*
Cl(1*)	12 (10)	764 (4)	4439 (6)	224 (5)*
Cl(2*)	-447 (13)	1851 (5)	3814 (8)	303 (9)*

<sup>a</sup> Asterisk indicates equivalent isotropic *U* defined as one-third of the trace of the orthogonalized *U*<sub>ij</sub> tensor.

scans of reflections spanning a range of  $2\theta$  values was applied. Systematically absent data suggested the monoclinic space group  $P2_1/n$  for both structures, and this was confirmed by successful refinement. Initial gold atom positions were determined from sharpened Patterson maps; all other non-hydrogen atoms were found in Fourier difference maps. Hydrogen atoms were included in the structures of **4** and **5** at calculated positions ( $\text{C-H} = 0.96$  Å) and were refined with fixed thermal parameters. All atoms other than hydrogens and phenyl group carbons were refined anisotropically. Phenyl groups were refined as regular hexagons ( $\text{C-C} = 1.395$  Å). An interstitial molecule of  $\text{CH}_2\text{Cl}_2$  was found in the structure of **4**, while a molecule of  $\text{CDCl}_3$  was found in the structure of **5** at positions of no chemical importance. Crystallographic data pertaining to **4** and **5** are listed in Table I. Atomic coordinates and equivalent isotropic thermal parameters for **4** and **5** are given in Tables II and III, respectively. Bond distances and angles are given in Tables IV and V, respectively.

### Results

The complexes **4** and **5** described here are the products of oxidation of **1** by ICl and Br<sub>2</sub>, respectively. The reactions of **1** with stoichiometric quantities of halogens give the trans/trans (about Au<sup>III</sup>) complexes  $[\text{Au}(\text{CH}_2)_2\text{PPh}_2]_2\text{X}_4$  ( $\text{X} = \text{Cl}$  (**2**),<sup>11</sup> Br (**3**)<sup>3b</sup>). The same products are obtained even with excess of halogens, provided that the reaction time does not exceed a few hours. The reactions<sup>3c</sup> of Au<sup>II</sup> complexes  $[\text{Au}(\text{CH}_2)_2\text{PPh}_2]_2\text{XY}$  ( $\text{Y} = \text{halogen or alkyl group}$ ) as well as the reaction of the "A-frame" type complex  $(\mu-\text{CH}_2)[\text{Au}(\text{CH}_2)_2\text{PPh}_2]_2\text{Br}_2$  with ICl also

- (2) (a) Fackler, J. P., Jr.; Basil, J. D. *Organometallics* **1982**, *1*, 871. (b) Murray, H. H.; Fackler, J. P., Jr.; Basil, J. D. *Organometallics* **1984**, *3*, 821. (c) Murray, H. H.; Fackler, J. P., Jr.; Mazany, A. M. *Organometallics* **1984**, *3*, 1310. (d) Murray, H. H.; Fackler, J. P., Jr.; Trzcinska-Bancroft, B. *Organometallics* **1985**, *4*, 1633. (e) Murray, H. H.; Mazany, A. M.; Fackler, J. P., Jr. *Organometallics* **1985**, *4*, 154. (f) Murray, H. H.; Fackler, J. P., Jr.; Tocher, D. A. *J. Chem. Soc., Chem. Commun.* **1985**, 1278. (g) Murray, H. H.; Fackler, J. P., Jr. *Inorg. Chim. Acta* **1986**, *115*, 207. (h) Murray, H. H.; Fackler, J. P., Jr.; Porter, L. C.; Mazany, A. M. *J. Chem. Soc., Chem. Commun.* **1986**, 321. (i) Porter, L. C.; Fackler, J. P., Jr. *Acta Crystallogr.* **1986**, *C42*, 1128. (j) Murray, H. H.; Fackler, J. P., Jr.; Mazany, A. M.; Porter, L. C.; Shain, J.; Falvello, L. R. *Inorg. Chim. Acta* **1986**, *114*, 171. (k) Porter, L. C.; Fackler, J. P., Jr. *Acta Crystallogr.* **1987**, *C43*, 29. (l) Porter, L. C.; Fackler, J. P., Jr. *Acta Crystallogr.* **1987**, *C43*, 587. (m) Trzcinska-Bancroft, B.; Khan, Md.; N. I.; Fackler, J. P., Jr. *Organometallics* **1988**, *7*, 993.
- (3) (a) Porter, L. C.; Murray, H. H.; Fackler, J. P., Jr. *Acta Crystallogr.* **1987**, *C43*, 877. (b) Dudis, D. S.; Fackler, J. P., Jr. *Inorg. Chem.* **1985**, *24*, 3758. (c) Murray, H. H.; Porter, L. C.; Fackler, J. P., Jr.; Raptis, R. G. *J. Chem. Soc., Dalton Trans.* **1988**, 2669.
- (4) Raptis, R. G.; Murray, H. H.; Porter, L. C.; Fackler, J. P., Jr. *Organometallics*, submitted for publication.
- (5) Jandik, P.; Schubert, H.; Schmidbauer, H. *Angew. Chem., Int. Ed. Engl.* **1982**, *21*, 73.
- (6) Stein, J.; Fackler, J. P., Jr.; Pappas; Chen, H. W. *J. Am. Chem. Soc.* **1981**, *103*, 2192.
- (7) Raptis, R. G.; Fackler, J. P., Jr.; Murray, H. H.; Porter, L. C. *Inorg. Chem.* **1989**, *28*, 4057.
- (8) Porter, L. C.; Knachel, H.; Fackler, J. P., Jr. *Acta Crystallogr.* **1986**, *C42*, 1125.
- (9) Heinrich, D. D. Ph.D. Dissertation, Texas A&M University, College Station, TX, 1987.
- (10) Fackler, J. P., Jr.; Trzcinska-Bancroft, B. *Organometallics* **1985**, *4*, 1891.

(11) Raptis, R. G.; Fackler, J. P., Jr. Unpublished results.

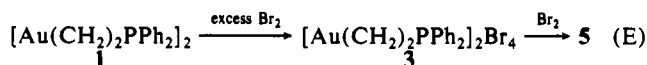
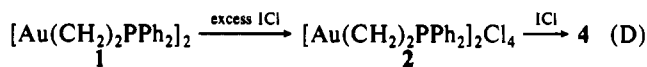
**Table III.** Atomic Coordinates ( $\times 10^4$ ) and Isotropic Thermal Parameters ( $\text{\AA}^2 \times 10^3$ ) for  $\text{Br}_3\text{Au}[\mu\text{-(CH}_2\text{)}_2\text{PPh}_2\text{]AuBr}_2(\text{CH}_2\text{PPh}_2\text{CH}_2\text{Br})\cdot\text{CDCl}_3$  (**5**)

atom	x	y	z	$U_{\text{iso}}^a$
Au(1)	9510 (2)	1773 (1)	8659 (1)	51 (1)*
Au(2)	13286 (2)	56 (1)	7663 (1)	51 (1)*
Br(1)	7996 (5)	2562 (2)	8753 (4)	96 (3)*
Br(2)	7729 (4)	1104 (2)	8516 (3)	78 (2)*
Br(3)	11371 (5)	2403 (2)	8884 (4)	92 (3)*
Br(4)	13354 (5)	72 (2)	6167 (3)	97 (3)*
Br(5)	13167 (4)	32 (2)	9159 (3)	82 (2)*
Br(6)	16584 (5)	-701 (2)	6192 (4)	91 (3)*
P(1)	10947 (11)	1002 (4)	7464 (7)	53 (5)*
P(2)	15803 (10)	-841 (4)	7934 (7)	50 (5)*
C(1)	10678 (42)	1135 (16)	8585 (23)	71 (19)*
C(2)	11239 (34)	251 (12)	7347 (32)	78 (21)*
C(15)	15385 (33)	-138 (15)	8012 (27)	63 (18)*
C(16)	15540 (35)	-1068 (13)	6830 (26)	63 (19)*
Cl(1)	10285 (15)	715 (6)	4525 (8)	115 (7)*
Cl(2)	9690 (22)	1872 (8)	4297 (12)	185 (12)*
Cl(3)	9567 (25)	1189 (8)	2859 (11)	210 (13)*
C(29)	9197 (28)	1198 (8)	3888 (12)	461 (110)*
C(4)	13384 (26)	1542 (10)	7873 (13)	59 (12)
C(5)	14484 (26)	1790 (10)	7663 (13)	75 (13)
C(6)	14500 (26)	1885 (10)	6803 (13)	62 (12)
C(7)	13415 (26)	1732 (10)	6154 (13)	83 (15)
C(8)	12314 (26)	1484 (10)	6364 (13)	61 (12)
C(3)	12299 (26)	1389 (10)	7224 (13)	47 (11)
C(10)	9136 (21)	1750 (10)	6483 (16)	59 (12)
C(11)	7929 (21)	1903 (10)	5949 (16)	63 (13)
C(12)	6967 (21)	1497 (10)	5653 (16)	49 (11)
C(13)	7212 (21)	937 (10)	5890 (16)	62 (13)
C(14)	8419 (21)	784 (10)	6424 (16)	72 (14)
C(9)	9381 (21)	1190 (10)	6720 (16)	57 (12)
C(18)	17938 (26)	-1496 (10)	8503 (18)	95 (17)
C(19)	19253 (26)	-1606 (10)	8903 (18)	71 (14)
C(20)	20105 (26)	-1164 (10)	9224 (18)	83 (15)
C(21)	19641 (26)	-614 (10)	9144 (18)	72 (14)
C(22)	18326 (26)	-504 (10)	8744 (18)	70 (14)
C(17)	17475 (26)	-945 (10)	8423 (18)	70 (14)
C(24)	13913 (28)	-1642 (11)	7995 (14)	79 (15)
C(25)	13187 (28)	-1985 (11)	8425 (14)	100 (17)
C(26)	13422 (28)	-1969 (11)	9321 (14)	89 (16)
C(27)	14383 (28)	-1610 (11)	9786 (14)	90 (16)
C(28)	15109 (28)	-1267 (11)	9356 (14)	84 (15)
C(23)	14874 (28)	-1283 (11)	8461 (14)	53 (12)

<sup>a</sup> Asterisk indicates equivalent isotropic  $U$  defined as one-third of the trace of the orthogonalized  $U_{ij}$  tensor.

give *trans/trans*- $[\text{Au}(\text{CH}_2)_2\text{PPh}_2]_2\text{Cl}_4$  (**2**). It is, therefore, assumed that the reactions D and E of Scheme II proceed by formation, as a first step, of the tetrahalide complexes **2** and **3**, respectively, followed by oxidation (and cleavage) of a  $\text{Au}^{\text{III}}\text{-CH}_2$  bond. However, reaction E is very slow (**5** is a minor product even after several weeks of reaction), while reaction D, which employs the polar reagent ICl, gives **4** in good yield in a few hours.

#### Scheme II



#### Discussion

The fact that the oxidation of **2** by ICl gives a product in which the chloride is bonded to gold while the iodide is bonded to the ylide suggests either a concerted mechanism in the reaction step or formation of a nonlabile  $\text{Au-Cl}$  bond. The isostructural complexes **4** and **5** consist of two gold(III) atoms bridged by an ylide ligand, while the second, halogenated ylide is monodentate. These are the products of the opening of the eight-membered ( $-\text{Au-C-P-C-}$ )<sub>2</sub> organogold ring by cleavage of a gold-carbon bond. The opening of the ring causes the gold centers to move away from each other. The  $\text{Au}\cdots\text{Au}$  distance is 6.0548 (8)  $\text{\AA}$  for **4** and 6.126 (2)  $\text{\AA}$  for **5**. The  $\text{Au}^{\text{III}}$  centers are four-coordinate with small

**Table IV.** Selected Distances ( $\text{\AA}$ ) and Angles (deg) for  $\text{Cl}_3\text{Au}[\mu\text{-(CH}_2\text{)}_2\text{PPh}_2]_2\text{AuCl}_2\text{PPh}_2\text{CH}_2\text{I}\cdot\text{CH}_2\text{Cl}_2$  (**4**)

Distances			
Au(1) $\cdots$ Au(2)	6.0548 (8)	P(1)-C(1)	1.797 (16)
Au(1)-Cl(1)	2.263 (5)	P(1)-C(2)	1.799 (16)
Au(1)-Cl(2)	2.357 (5)	P(2)-C(3)	1.781 (14)
Au(1)-Cl(3)	2.282 (5)	P(2)-C(4)	1.796 (14)
Au(2)-Cl(4)	2.272 (5)	P(1)-C(16)	1.788 (13)
Au(2)-Cl(5)	2.282 (5)	P(1)-C(26)	1.783 (9)
Au(1)-C(1)	2.052 (16)	P(2)-C(36)	1.786 (11)
Au(2)-C(2)	2.095 (15)	P(2)-C(46)	1.771 (12)
Au(2)-C(3)	2.112 (15)	C(4)-I	2.112 (16)
Angles			
Cl(1)-Au(1)-Cl(2)	91.2 (2)	C(2)-P(1)-C(16)	108.4 (7)
Cl(1)-Au(1)-Cl(3)	176.4 (2)	C(2)-P(1)-C(26)	110.0 (16)
Cl(2)-Au(1)-Cl(3)	92.2 (2)	C(16)-P(1)-C(26)	108.5 (5)
Cl(1)-Au(1)-C(1)	88.8 (5)	C(3)-P(2)-C(4)	112.5 (7)
Cl(2)-Au(1)-C(1)	179.3 (4)	C(3)-P(2)-C(36)	110.6 (6)
Cl(3)-Au(1)-C(1)	87.8 (5)	C(3)-P(2)-C(46)	110.2 (7)
Cl(4)-Au(2)-Cl(5)	178.6 (2)	C(4)-P(2)-C(36)	108.3 (6)
Cl(4)-Au(2)-C(2)	89.6 (5)	C(4)-P(2)-C(46)	106.1 (6)
Cl(4)-Au(2)-C(3)	90.0 (5)	C(36)-P(2)-C(46)	108.5 (5)
Cl(5)-Au(2)-C(2)	89.4 (5)	Au(1)-C(1)-P(1)	113.3 (7)
Cl(5)-Au(2)-C(3)	91.1 (5)	Au(2)-C(2)-P(1)	112.0 (7)
C(1)-P(1)-C(2)	109.0 (8)	Au(2)-C(3)-P(2)	115.2 (7)
C(1)-P(1)-C(16)	112.8 (6)	P(2)-C(4)-I	114.1 (7)
C(1)-P(1)-C(26)	108.1 (6)		

**Table V.** Selected Distances ( $\text{\AA}$ ) and Angles (deg) for  $\text{Br}_3\text{Au}[\mu\text{-(CH}_2\text{)}_2\text{PPh}_2]_2\text{AuBr}_2(\text{CH}_2\text{PPh}_2\text{CH}_2\text{Br})\cdot\text{CDCl}_3$  (**5**)

Distances			
Au(1) $\cdots$ Au(2)	6.126 (2)	P(1)-C(1)	1.90 (4)
Au(1)-Br(1)	2.479 (6)	P(1)-C(2)	1.83 (3)
Au(1)-Br(2)	2.415 (5)	P(2)-C(15)	1.74 (4)
Au(1)-Br(3)	2.410 (5)	P(2)-C(16)	1.80 (4)
Au(2)-Br(4)	2.406 (6)	P(1)-C(3)	1.79 (3)
Au(2)-Br(5)	2.420 (5)	P(1)-C(9)	1.84 (2)
Au(1)-C(1)	1.97 (4)	P(2)-C(17)	1.75 (3)
Au(2)-C(2)	2.12 (3)	P(2)-C(23)	1.77 (2)
Au(2)-C(15)	2.18 (3)	C(16)-Br(6)	1.89 (4)
Angles			
Br(1)-Au(1)-Br(2)	91.4 (2)	C(2)-P(1)-C(3)	109 (2)
Br(1)-Au(1)-Br(3)	90.9 (3)	C(2)-P(1)-C(9)	108 (1)
Br(2)-Au(1)-Br(3)	176.0 (2)	C(3)-P(1)-C(9)	111 (1)
Br(1)-Au(1)-C(1)	179 (1)	C(15)-P(2)-C(16)	112 (2)
Br(2)-Au(1)-C(1)	87 (1)	C(15)-P(2)-C(17)	110 (1)
Br(3)-Au(1)-C(1)	90 (1)	C(15)-P(2)-C(23)	112 (2)
Br(4)-Au(2)-Br(5)	178.7 (2)	C(16)-P(2)-C(17)	108 (2)
Br(4)-Au(2)-C(2)	91 (1)	C(16)-P(2)-C(23)	108 (1)
Br(4)-Au(2)-C(15)	90 (1)	C(17)-P(2)-C(23)	107 (1)
Br(5)-Au(2)-C(2)	88 (1)	Au(1)-C(1)-P(1)	114 (2)
Br(5)-Au(2)-C(15)	91 (1)	Au(2)-C(2)-P(1)	112 (2)
C(1)-P(1)-C(2)	109 (2)	Au(2)-C(15)-P(2)	116 (2)
C(1)-P(1)-C(3)	114 (1)	P(2)-C(16)-Br(6)	115 (2)
C(1)-P(1)-C(9)	106 (2)		

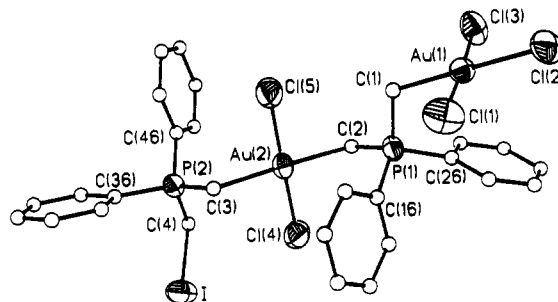


**Figure 1.** Drawing of the structure of **4**. Thermal ellipsoids have been drawn at the 50% probability level. Carbon atoms are of arbitrary radii for clarity. The solvent molecule is not shown.

deviations from an idealized square-planar geometry. For **4** (Figure 1), the cis angles range between 87.8 (5) and 92.2 (2)°, while the trans angles are between 176.4 (2) and 179.3 (4)°. For **5** (Figure 2), the corresponding ranges are 87 (1)–91.4 (2)° and

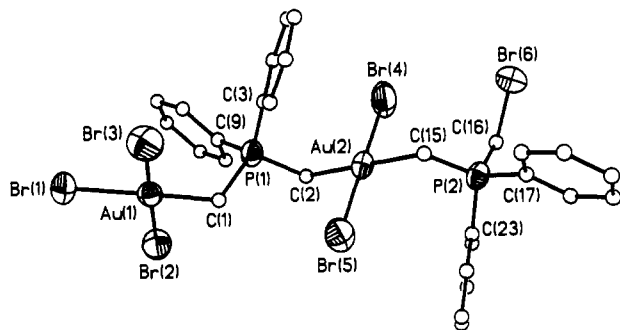


**Figure 2.** Drawing of the structure of **5**. Thermal ellipsoids have been drawn at the 50% probability level. Carbon atoms are of arbitrary radii for clarity. The solvent molecule is not shown.

176.0 (2)–179 (1)°. Nothing unusual is observed in the geometries of the ylide ligands. The gold–halogen bond lengths, particularly those of complex **5**, are of interest.

With regard to the gold–halogen bond lengths, we have recently described two conformers of the *trans/trans* complex **3**, one that crystallized<sup>3b</sup> in the space group *C2/c* with an interstitial molecule of  $\text{CDCl}_3$  and one that crystallized<sup>7</sup> in *P2<sub>1</sub>/c* with no solvent molecule. In the *C2/c* structure, two bromine atoms are tilted toward a semibringing position and the measured Au–Br bonds are 2.411 (3) and 2.440 (3) Å. However, in the *P2<sub>1</sub>/c* structure, a trigonal-bipyramidal distortion of the geometry of Au atoms is observed in which the Au–Br bond lengths are significantly longer, 2.535 (4) and 2.576 (4) Å. The latter distortion was attributed<sup>7</sup> to the intramolecular interaction of the two Au<sup>III</sup> atoms, which were separated by a 3.069 (2) Å distance.

The comparative study of the *C2/c* and *P2<sub>1</sub>/c* structures of **3** raised the question of choosing a standard Au<sup>III</sup>–Br bond length against which the *trans*–Br–Au–Br units can be compared. We believe that the bond lengths measured around Au(2) of structure **5** can be accepted as standard for a *trans*–Au<sup>III</sup>Br<sub>2</sub> bond. This

gold atom has a coordination identical with that of the gold atoms of **3**, two *trans* ylides and two *trans* bromides, while its geometry is not disturbed by any other interactions. The Au(2)–Br bonds measured in **5**, 2.406 (6) and 2.420 (5) Å, are in good agreement with the bond lengths of the *C2/c* structure of **3**, confirming our previous assumption that the latter bond lengths are not affected by intramolecular Br...Br interactions.

The Au(1)–Br(1) bond of **5**, *trans* to the ylide ligand and *cis* to the other bromides, is very long, 2.479 (6) Å, reflecting the *trans* influence of the  $-\text{CH}_2-$  group. The *cis/cis* isomer<sup>4</sup> of **3** also has long Au–Br bonds, 2.497 (4) and 2.487 (5) Å, as does as the *cis* side of the *cis/trans* complex<sup>3c</sup>  $[\text{Au}(\text{CH}_2)_2\text{PPh}_2]_2(\text{CH}_2\text{CF}_3)\text{Br}_3$ , 2.470 (3) and 2.476 (4) Å. Also, the Au–Cl bond lengths of **4** are in good agreement with the bond lengths measured in the structure of the *cis/trans* isomer<sup>3b</sup> of **2**. The *cis* side of the latter structure has Au–Cl bonds of 2.338 (9) and 2.360 (7) Å. The 2.357 (5) Å Au(1)–Cl(2) bond of **4** falls in this range, while the *trans* side of *cis/trans*-**2** has Au–Cl bonds of 2.295 (9) and 2.272 (9) Å, similar to the ones measured in the *trans*–AuCl<sub>2</sub> units of **4**.

We have mentioned (*vide supra*) that the reactions<sup>3c</sup> of ICl and Br<sub>2</sub> with the Au<sup>III</sup> A-frame complexes  $(\mu\text{-CH}_2)[\text{Au}(\text{CH}_2)_2\text{PPh}_2]_2\text{X}_2$  cleave the Au–( $\mu\text{-CH}_2$ ) bonds, not the Au–CH<sub>2</sub>(ylide) bonds, with formation of dihalomethanes. This preferential reactivity has been used<sup>11</sup> to synthesize mixed-ligand complexes such as *trans/trans*– $[\text{Au}(\text{CH}_2)_2\text{PPh}_2]_2(\text{CN})_2\text{X}_2$  (X = Cl, Br) obtained from the reaction of  $(\mu\text{-CH}_2)[\text{Au}(\text{CH}_2)_2\text{PPh}_2]_2(\text{CN})_2$  with ICl and Br<sub>2</sub>, respectively.

**Acknowledgment.** We acknowledge with thanks the financial support for this work from the National Science Foundation (Grant CHE8708625) and the Robert A. Welch Foundation.

**Supplementary Material Available:** Tables SI–SIX, listing crystallographic data, bond lengths, bond angles, anisotropic thermal parameters, and hydrogen positional parameters for **4** and **5** (11 pages); Tables SX and SXI, listing observed and calculated structure factors for **4** and **5** (59 pages). Ordering information is given on any current masthead page.

Contribution from the Groupe de Spectroscopie des Complexes Polymétalliques et de Métalloprotéines and Groupe Structure, Service de Physique, Département de Recherche Fondamentale (DRF) du Centre d'Etudes Nucléaires de Grenoble (CENG), 85X, Grenoble 38041, France, and Université Joseph Fourier, Grenoble, France

## Influence of a Phase Transition in the Solid State on the Structure of a Synthetic Iron–Sulfur Cubane

P. Excoffon,<sup>\*,†,‡</sup> J. Laugier,<sup>§</sup> and B. Lamotte<sup>\*,‡</sup>

Received July 23, 1990

The tetranuclear iron–sulfur cubane compound  $[\text{Bu}_4\text{N}]_2[\text{Fe}_4\text{S}_4(\text{SC}_6\text{H}_5)_4]$ , which is a good model for the active sites of ferredoxins, presents a phase transition at 243 K between two solid phases called phase I and phase II. The crystallographic structure of phase II having been previously described, we report here, in order to compare them, the structure of phase I at 233 K. Its space group is orthorhombic *P2<sub>1</sub>na*, with  $a = 11.888$  (5) Å,  $b = 23.21$  (1) Å,  $c = 22.22$  (1) Å,  $\alpha = \beta = \gamma = 90^\circ$ . The structure has been refined for 5866 reflections, 3697 of which were greater than  $2\sigma(I)$ . The final values are  $R = 0.044$ ,  $R_w = 0.057$ . The phase transition has been studied and is found to be of the first order. It presents a small hysteresis, and its total entropy gain is  $\Delta S = 7.5 \text{ J K}^{-1} \text{ mol}^{-1}$ . In the two phases and principally in phase I the cubane core is distorted from  $T_d$  symmetry, the distortion not being describable as a  $D_{2d}$  compression. The phase transition does not appear to be driven by the geometry changes appearing at the cubane core level. Rather, the origin of this phase transition must be due to an increase of disorder at the butyl ends of the counterions and to simultaneous changes of the orientations of the benzenethiolate ligands. Thus, we view the changes of geometry and symmetry appearing at the level of the cubane core as essentially shaped by its immediate environment, within the limits of plasticity that this structure admits.

### I. Introduction

Iron–sulfur cubanes are interesting clusters since they constitute the active site of numerous metalloproteins involved in electron-

transfer biological processes.<sup>1–3</sup> In order to understand their properties, Holm and co-workers<sup>4</sup> have created and studied ex-

<sup>†</sup> Université Joseph Fourier.

<sup>‡</sup> Groupe de Spectroscopie des Complexes Polymétalliques et de Métalloprotéines.

<sup>§</sup> Groupe Structure.

(1) Lovenberg, W., Ed. *Iron Sulfur Proteins* Academic Press: New York, 1977.

(2) Spiro, T. G., Ed. *Iron Sulfur Proteins* John Wiley and Sons, Inc.: New York, 1982.

(3) *Iron Sulfur Protein Research*; Matsubara, Hiroshi, Katsube, Yukiteru, Wada, Keishiro, Eds.; Japan Scientific Societies Press: Tokyo, 1987.